

Potential Applicability of Brillouin Scattering in Partially Chlorinated Polymer Optical Fibers to High-Precision Temperature Sensing

Kazunari Minakawa, Neisei Hayashi, Yosuke Mizuno, and Kentaro Nakamura

Precision and Intelligence Laboratory, Tokyo Institute of Technology, Yokohama 226-8503, Japan

Received February 22, 2013; accepted April 2, 2013; published online April 18, 2013

Using the ultrasonic pulse–echo technique, we estimate the Brillouin frequency shift (BFS) and its temperature dependence in partially chlorinated graded-index polymer optical fibers (PCGI-POFs), which have high thermal stability compared with other POFs. At 1550 nm, the estimated BFS is ~4.43 GHz with its temperature coefficient of approximately –6.9 MHz/K, which is ~5.8 times as large as that in silica fibers. Since the fracture strain is ~3.0% (mostly in the elastic region), the BFS dependence on strain in PCGI-POFs cannot be estimated by this technique. These results indicate that Brillouin scattering in PCGI-POFs has a big potential for distributed high-precision temperature sensing.

© 2013 The Japan Society of Applied Physics

Brillouin scattering in optical fibers¹⁾ has been exploited to develop a remarkably wide variety of devices and systems, such as lasers,²⁾ signal processors,³⁾ phase conjugators,⁴⁾ slow light generators,⁵⁾ optical storages,⁶⁾ core aligners,⁷⁾ optical compressors,⁸⁾ delay lines,⁹⁾ coolers,¹⁰⁾ and gyroscopes.¹¹⁾ Distributed strain and temperature sensing is also one of its most important applications,^{12–17)} and extensive research has been performed for the past several decades. In conventional fiber-optic Brillouin sensors, their sensing heads are composed of glass optical fibers (GOFs) such as silica single-mode fibers (SMFs), which cannot withstand strains of larger than several percent. To extend the applicable strain range, we have been studying Brillouin sensors based on polymer optical fibers (POFs).^{18–21)} POFs are generally so flexible compared with GOFs that they can withstand strains of over 50%. Besides, they have many attractive features such as low cost, ease of installation, and high safety.

Commercially available POFs are classified into three: poly(methyl methacrylate)-based (PMMA-) POFs, perfluorinated graded-index (PFGI-) POFs, and partially chlorinated (PC) GI-POFs. Brillouin scattering in PFGI-POFs with relatively low loss at 1550 nm has already been observed and investigated.^{18,19)} Brillouin scattering in PMMA-POFs cannot be directly observed due to their large core diameter and extremely high loss at 1550 nm, but their Brillouin properties have been estimated using the ultrasonic pulse–echo technique.^{20,21)} PCGI-POFs have recently attracted considerable attention because of their low propagation loss at the 650–700/750–800 nm region as well as their high thermal resistance of up to ~100 °C (cf. 70 °C in other POFs),^{22,23)} which enables the implementation of Brillouin sensors with a wide temperature range. However, since their propagation loss is high at 1550 nm, where various devices are available for Brillouin detection with high frequency resolution, Brillouin scattering in PCGI-POFs has not been observed yet.

In this paper, we measure the acoustic velocity in a PCGI-POF using the ultrasonic pulse–echo technique, based on which the Brillouin frequency shift (BFS) and its temperature dependence are estimated. The BFS is calculated to be ~4.43 GHz at 1550 nm. Its temperature coefficient is approximately –6.9 MHz/K, the absolute value of which is ~1.7 times as large as that of a PFGI-POF. The fracture strain of the PCGI-POF is ~3.0% (basically in the elastic region), and so the BFS dependence on strain cannot be estimated by this technique. These measurement results

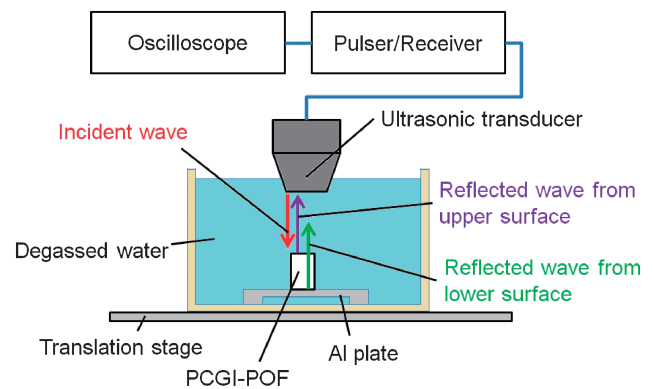


Fig. 1. Experimental setup for acoustic velocity measurement in PCGI-POF.

predict that the Brillouin scattering in PCGI-POFs is highly suitable for the implementation of high-precision temperature-sensing systems.

When pump light is injected into an optical fiber, backscattered light called Stokes light is generated due to the interaction with acoustic phonons, and it propagates in the direction opposite to the pump light. This phenomenon is called Brillouin scattering.¹⁾ The central frequency of the Stokes light spectrum, called the Brillouin gain spectrum (BGS), shifts to a lower frequency than the pump frequency. The magnitude of this frequency downshift is called BFS, which is expressed by¹⁾

$$\text{BFS} = \frac{2nv_A}{\lambda_p}, \quad (1)$$

where n is the core refractive index, v_A is the acoustic velocity in the fiber, and λ_p is the pump wavelength. Thus, by measuring v_A in a target fiber with known n , the BFS at an arbitrary pump wavelength can be estimated.

We employed a 1.00-mm-long PCGI-POF sample with an outer diameter of 750 μm, a core diameter of 120 μm, and a core refractive index of ~1.52. Both ends of the sample were carefully polished with 3 μm alumina powders. Figure 1 depicts the experimental setup for measuring the acoustic velocity in the PCGI-POF sample, which is basically the same as that in Ref. 20. A pulsed converging ultrasonic wave with a center frequency of ~20 MHz generated with a focus-type transducer (Panametrics M316) connected to a pulser/receiver (Panametrics 5900PR) was launched into the sample fixed on an aluminum plate in degassed water.

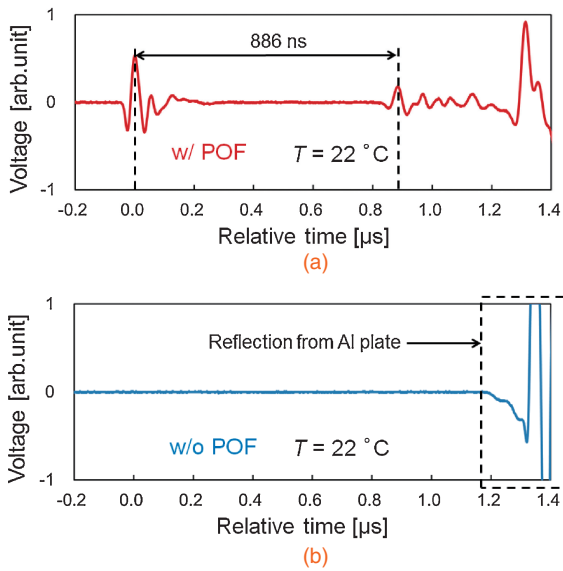


Fig. 2. Measured echo waveforms (a) with and (b) without PCGI-POF at 22°C.

The temperature of the degassed water was controlled with a heater. The effective diameter of the focused wave was 720 μm. The reflected waves from the top and bottom of the sample were detected with the same transducer and observed with an oscilloscope. Using the time delay between the observed reflected waves and the length of the sample, the acoustic velocity can be calculated.

Figures 2(a) and 2(b) show the measured echo waveforms at room temperature (22 °C) with and without the PCGI-POF sample on the stage, respectively. In Fig. 2(a), the clear peak, where the relative time was defined as 0 μs, represents the reflected wave from the top of the sample; the relatively small peak at ~0.9 μs indicates the reflected wave at its bottom. The large fluctuations at ~1.3 μs were caused by the reflection from the stage surface, because similar fluctuations were observed without the sample as shown in Fig. 2(b). Thus, we obtained a time delay of 886 ns, with which, using the sample length (= 1.00 mm), the acoustic velocity in the PCGI-POF sample was calculated to be 2.26 km/s. Then, using Eq. (1), the BFS in the PCGI-POF, which is inversely proportional to the pump wavelength, was also calculated to be ~4.43 GHz at 1550 nm (~10.57 GHz at 650 nm). This value is 0.82 times the BFS in PMMA-POFs,²⁰ which indicates that the acoustic velocity or BFS can be moderately controlled by adjusting the doping concentration of chlorine to PMMA-POFs. In the meantime, since the BFS in the PCGI-POF is 1.6 times as high as that in PFGI-POFs,¹⁸ we can expect that the signal-to-noise (SNR) deterioration caused by Rayleigh noise²⁴ will be mitigated by employing PCGI-POFs.

Next, by changing the temperature of the sample in the range from 20 to 80 °C, the BFS dependence on temperature in a PCGI-POF at 1550 nm was estimated, as shown in Fig. 3. The refractive-index dependence on temperature was not taken into account, under the assumptions that its coefficient is as negligibly small as that in bulk PMMA.²⁵ The hollow-circle and solid-square points were measured with increasing and decreasing temperature, respectively. In this temperature range, the BFS showed a linear change with

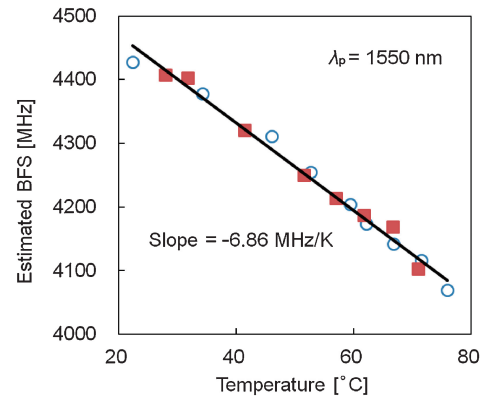


Fig. 3. Estimated BFS in PCGI-POF at 1550 nm as a function of increasing (hollow circles) and decreasing (solid squares) temperature.

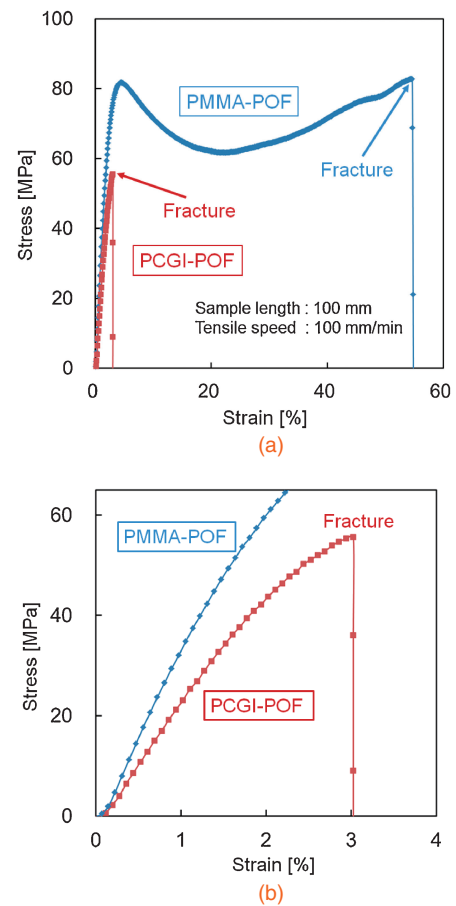


Fig. 4. (a) Measured stress–strain curves of PCGI-POF and PMMA-POF,⁷ and (b) their magnified view in the range below 4% strain.

temperature with no hysteresis. The temperature coefficient was approximately -6.9 MHz/K, the absolute value of which is ~1.7 times as large as that of PFGI-POFs¹⁹ (and even ~5.8 times as large as that of silica SMFs²⁶). Thus, Brillouin scattering in PCGI-POFs seems to be potentially applicable to high-precision temperature sensing.

Finally, to estimate the BFS dependence on strain, we investigated a stress–strain curve of a 100-mm-long PCGI-POF using a tension tester (Shimadzu AG-500N), as shown in Fig. 4(a), where a stress–strain curve of a 100-mm-long PMMA-POF²¹ is also shown for comparison. The tensile

speed was set to 100 mm/min (Note that no significant change was observed in the stress–strain curve of the PCGI-POF when the tensile speed was reduced to 12 mm/min.). The fracture strain of the PCGI-POF was $\sim 3.0\%$, which is much smaller than that of the PMMA-POF ($\sim 55\%$). The magnified view of the stress–strain curve of the PCGI-POF is shown in Fig. 4(b). Its fracture strain seems to be even smaller than the upper yield point ($\sim 4.5\%$ in the PMMA-POF), indicating that PCGI-POFs lie mainly in the elastic region, that their BFS dependence on strain cannot be estimated by the ultrasonic pulse–echo technique, and that they are not suitable for large-strain sensing with a so-called memory effect exploiting plastic deformation.²⁷⁾

In conclusion, the acoustic velocity in a PCGI-POF was measured using the ultrasonic pulse–echo technique, and the BFS was estimated together with its temperature dependence. The acoustic velocity at room temperature was 2.26 km/s, corresponding to the BFS of ~ 4.43 GHz at 1550 nm and ~ 10.57 GHz at 650 nm. The coefficient of its temperature dependence was as large (absolute value) as -6.9 MHz/K at 1550 nm, which is ~ 1.7 times as high as that of a PFGI-POF. By measuring the stress–strain curve of the PCGI-POF, its fracture strain was found to be $\sim 3.0\%$, which is much smaller than those of other POFs. Thus, although PCGI-POFs do not appear to be suitable for large-strain sensing, we believe that they will be of great use in developing distributed Brillouin temperature sensors, exploiting their high thermal stability and high-precision temperature-sensing capability.

Acknowledgments We are indebted to Sekisui Chemical Co., Ltd., for providing us with PCGI-POF samples. We are also grateful to Professor H. Hosoda at Tokyo Institute of Technology for lending us the tension tester. This work was partially supported by a Grant-in-Aid for Research Activity Start-up (24860029) from the Japan Society for the Promotion of Science (JSPS), and by

research grants from the JFE 21st Century Foundation, the General Sekiyu Foundation, and the Iwatani Naoji Foundation.

- 1) G. P. Agrawal: *Nonlinear Fiber Optics* (Academic Press, San Diego, CA, 2001).
- 2) G. Wang, L. Zhan, J. Liu, T. Zhang, J. Li, L. Zhang, J. Peng, and L. Yi: *Opt. Lett.* **38** (2013) 19.
- 3) S. Norcia, S. Tonda-Goldstein, D. Dolfi, J.-P. Huignard, and R. Frey: *Opt. Lett.* **28** (2003) 1888.
- 4) E. A. Kuzin, M. P. Petrov, and B. E. Davydenko: *Opt. Quantum Electron.* **17** (1985) 393.
- 5) K. Y. Song, M. Herráez, and L. Thévenaz: *Opt. Express* **13** (2005) 82.
- 6) Z. Zhu, D. J. Gauthier, and R. W. Boyd: *Science* **318** (2007) 1748.
- 7) Y. Mizuno and K. Nakamura: *J. Lightwave Technol.* **29** (2011) 2616.
- 8) Y. Okawachi and A. L. Gaeta: *Nat. Photonics* **6** (2012) 274.
- 9) W. Zou, Z. He, and K. Hotate: *Appl. Phys. Express* **3** (2010) 012501.
- 10) G. Bahl, M. Tomes, F. Marquardt, and T. Carmon: *Nat. Phys.* **8** (2012) 203.
- 11) F. Zarinetchi, S. P. Smith, and S. Ezekiel: *Opt. Lett.* **16** (1991) 229.
- 12) P. Dragic, T. Hawkins, P. Foy, S. Morris, and J. Ballato: *Nat. Photonics* **6** (2012) 627.
- 13) T. Horiguchi and M. Tateda: *J. Lightwave Technol.* **7** (1989) 1170.
- 14) T. Kurashima, T. Horiguchi, H. Izumita, S. Furukawa, and Y. Koyamada: *IEICE Trans. Commun.* **E76-B** (1993) 382.
- 15) D. Garus, K. Krebber, F. Schliep, and T. Gogolla: *Opt. Lett.* **21** (1996) 1402.
- 16) K. Hotate and T. Hasegawa: *IEICE Trans. Electron.* **E83-C** (2000) 405.
- 17) Y. Mizuno, W. Zou, Z. He, and K. Hotate: *Opt. Express* **16** (2008) 12148.
- 18) Y. Mizuno and K. Nakamura: *Appl. Phys. Lett.* **97** (2010) 021103.
- 19) Y. Mizuno and K. Nakamura: *Opt. Lett.* **35** (2010) 3985.
- 20) N. Hayashi, Y. Mizuno, D. Koyama, and K. Nakamura: *Appl. Phys. Express* **4** (2011) 102501.
- 21) N. Hayashi, Y. Mizuno, D. Koyama, and K. Nakamura: *Appl. Phys. Express* **5** (2012) 032502.
- 22) H. Yoshida and Y. Koike: *Proc. POF2012*, p. 266.
- 23) K. Koike, F. Mikes, Y. Okamoto, and Y. Koike: *J. Polym. Sci., Part A* **47** (2009) 3352.
- 24) Y. Mizuno, N. Hayashi, and K. Nakamura: *Electron. Lett.* **49** (2013) 56.
- 25) J. Brandrup, E. H. Immergut, and E. A. Gulke: *Polymer Handbook* (Wiley, New York, 1999).
- 26) T. Kurashima, T. Horiguchi, and M. Tateda: *Appl. Opt.* **29** (1990) 2219.
- 27) K. Nakamura, I. R. Husdi, and S. Ueha: *Proc. SPIE* **5855** (2005) 807.